

Wilson loops for triangular contours with circular edges

Harald Dorn ¹

*Institut für Physik und IRIS Adlershof, Humboldt-Universität zu Berlin,
Zum Großen Windkanal 6, D-12489 Berlin, Germany*

Abstract

We calculate Wilson loops in lowest order of perturbation theory for triangular contours whose edges are circular arcs. Based on a suitable disentanglement of the relations between metrical and conformal parameters of the contours, the result fits perfectly in the structure predicted by the anomalous conformal Ward identity. The conformal remainder function depends in the generic 4D case on three cusp and on three torsion angles. The restrictions on these angles imposed by the closing of the contour are discussed in detail and also for cases in 3D and 2D.

¹dorn@physik.hu-berlin.de

1 Introduction

In a recent paper [1] we have derived anomalous conformal Ward identities for Wilson loops along polygon-like contours, whose edges are made of circular arcs. They enforce a factorised structure, with one factor depending on the distances between the corners and the cusp anomalous dimensions, just in the same way as in correlation functions of local conformal operators with their conformal dimensions. The second factor is a remainder, depending only on conformal invariant parameters characterising the circular polygon. These parameters are the cusp angles, torsion angles and for more than three corners the usual cross ratios of the corner points.

Certainly it would have been useful to illustrate and underpin this general result by an explicit calculation. But it turned out to be a bit tricky to disentangle the relevant equations between the involved metrical and conformal parameters in short time and to extract the finite piece remaining after subtraction of the UV divergent cusp terms.

The aim of this paper is to fill this gap by a lowest order calculation of the remainder function for the triangle with circular edges in Euclidean $\mathcal{N} = 4$ SYM. This we will do for the generic case which winds in full 4D space and comment also on triangles in 3D as well as on the planar situation.

As a side effect, thereby we generate a rare example of a Wilson loop calculation for a contour not restricted to a subspace. The only other examples seem to be the Wilson loops for light-like polygons studied a lot in connection with the duality to scattering amplitudes [2], [3]. But there the contours are fixed by their corners and one has no parameters for some additional freedom of the edges. Wilson loops for toroidal contours winding in 3D have been studied in [4].

The Maldacena-Wilson loops for planar circular triangles have been studied non-perturbatively in [5], but in a special limit which involves large imaginary angles for the coupling of the scalars. For the treatment at strong coupling via AdS/CFT of generic smooth contours winding in full 4D the local conformal characteristics of the contour have been related to the boundary data of the Pohlmeyer fields in [6].

Wilson loops for triangles with straight edges have been used in QCD for applications to baryon phenomenology, see e.g. [7–9] and references therein. There is also recent work on the large size behaviour for standard planar polygons with straight edges [10].

For a first visualisation of the contour under consideration we show fig.1, taken from [1]. For obvious reasons it is a 3D object. In the generic 4D case one has eleven related independent metrical invariants [1]. As those can be chosen the three distances between the corners X_j

$$D_{ij} = |X_i - X_j|, \quad (1)$$

the radii R_j of the three edges, the three distances between the centers of circular edges and two of the distances between a corner X_j and the center of the opposite circular edge Z_j . Furthermore, there are only six conformal invariants, three angles α_j and three angles β_j , where α_j is the cusp angle at corner X_j and β_j the angle between

the circumcircle and the edge number j . Due to their meaning in our geometrical setting, all angles α_j and β_j are a priori restricted to the interval $(0, \pi)$. In the planar case the β_j are fixed by the cusp angles, but as soon as they vary independently from these constraints, the contour winds out of the plane fixed by the corners.² Our task will be to find a representation of the Wilson loop in terms of the set $(D_{ij}, \alpha_j, \beta_j)$.

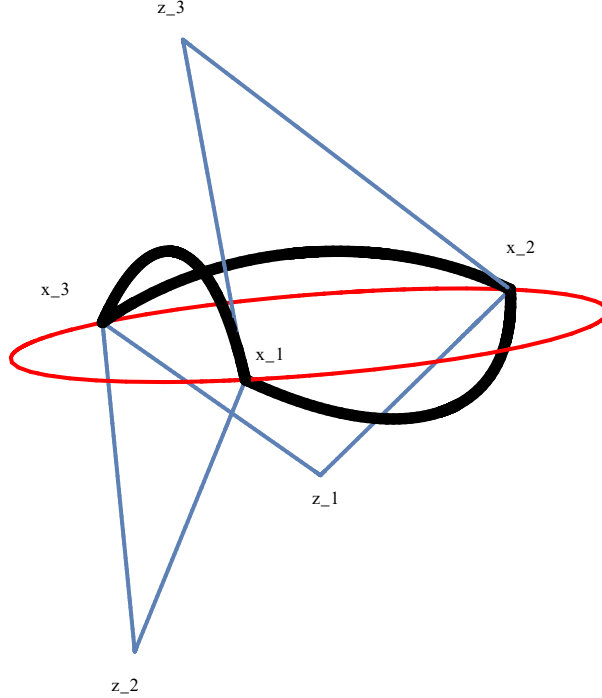


Figure 1: A triangle with corners X_1, X_2, X_3 and circular edges is shown in black. The corresponding circum circle is depicted in red. The blue lines are the radii connecting the corners with the centers related to the circular edges.

The Maldacena-Wilson loop is defined by

$$\mathcal{W} = \left\langle \frac{1}{N} \text{tr} \text{P exp} \int (iA_\mu \dot{x}^\mu + |\dot{x}| \phi_i \theta^i) dt \right\rangle . \quad (2)$$

Let us consider here only the case with constant θ^i along the whole contour. In lowest order we have³

$$\log \mathcal{W} = \frac{g^2 C_F}{4\pi^2} I + \mathcal{O}(g^4) , \quad (3)$$

$$I = I^{\text{scalar}} - I^{\text{vector}} = \frac{1}{2} \int \int \frac{|\dot{x}_1| |\dot{x}_2| - \dot{x}_1 \dot{x}_2}{(x_1 - x_2)^2 + a^2} dt_1 dt_2 , \quad (4)$$

understood as limit $a \rightarrow 0$ after subtraction of the divergent pieces.

This regularisation has been used in the first paper on the cusp anomalous dimension for the pure gauge field case [11] and also in the first paper on the supersymmetric

²For that reason we call them torsion angles.

³ $C_F = \frac{N^2 - 1}{2N}$ for $SU(N)$ gauge group.

case [12]. Later calculations of higher orders have mainly used dimensional regularisation. Note that for that purpose they could use straight edges. Our choice seems technically more convenient for the evaluation of the finite piece for a curved contour.

According to [1] the Wilson loop for a triangle with circular edges as in fig.1 has the following structure ⁴

$$\mathcal{W} = D_{12}^{\Gamma_3 - \Gamma_1 - \Gamma_2} D_{23}^{\Gamma_1 - \Gamma_2 - \Gamma_3} D_{13}^{\Gamma_2 - \Gamma_1 - \Gamma_3} \Omega(\alpha_j, \beta_j) . \quad (5)$$

$\Gamma_j = \Gamma(\alpha_j)$ are the cusp anomalous dimensions. They are ⁵

$$\Gamma(\alpha) = \frac{g^2 C_F}{4\pi^2} \gamma(\alpha) + \mathcal{O}(g^4) , \quad (6)$$

with

$$\gamma(\alpha) = -(\pi - \alpha) \frac{1 + \cos\alpha}{\sin\alpha} \quad \text{or} \quad \gamma(\alpha) = -(1 + (\pi - \alpha)\cot\alpha) \quad (7)$$

for the Maldacena-Wilson loop (2) with smooth contour in the internal space or the Wilson loop for pure gauge fields, respectively.

The remainder function Ω depends on three, five, or six independent conformal invariants in $D = 2$, $D = 3$, or $D = 4$ dimensions, respectively. As these conformal invariants can be chosen the 3 cusp angles α_j in $D = 2$, due to a closing condition five angles out of the three cusp angles and the three torsion angles β_j in $D = 3$ and all six angles without a local constraint in $D = 4$.

In calculating (4) one has to add the three pieces where $x_1(t_1)$ and $x_2(t_2)$ are on the same edge and the three pieces where they are on the adjacent edges of one of the corner points, i.e.

$$I = \sum_{j=1}^3 (E_j + C_j) . \quad (8)$$

Only after taking into account the condition that the single terms in (8) combine to a closed contour, one can organise the dependence on metrical and conformal invariants in a manner required to fit (5).

To illustrate this issue, and as a warm up, let us consider in the next section the limiting case of a standard triangle with straight edges (then we have only 2 conformal invariants, since $\sum \alpha_j = \pi$).

In the generic case there are more metrical invariants beyond the D_{ij} 's, and the relations between them and the conformal invariants are far more involved. Therefore, we use in section 3 conformal invariance to calculate the corner building blocks C_j in a suitable conformal frame. This allows from the beginning a parameterisation with maximal use of conformal invariants.⁶

Several technical calculations are sketched in appendices.

⁴As in [1] we neglect an overall factor $\mu^{-\sum \Gamma_j}$, depending on the RG scale μ .

⁵ α chosen as the opening angle of a cusp, i.e. $\alpha = \pi$ as smooth case.

⁶For circular triangles in a plane there has been used in [5] a clever parameterisation of the original geometry in terms of the corner points and cusp angles, without using the radii. We do not know a suitable extension beyond the planar case.

2 The standard triangle with straight edges

Due to the straight edges, in this case the scalar and vector contributions are trivially related

$$C_j^{\text{vector}} = -\cos\alpha_j C_j^{\text{scalar}}, \quad E_j^{\text{vector}} = E_j^{\text{scalar}}. \quad (9)$$

For the corner term, e.g. for the corner at X_3 we have

$$C_3^{\text{scalar}} = \int_0^{D_{23}} dt_1 \int_0^{D_{13}} dt_2 \frac{1}{t_1^2 + t_2^2 - 2t_1 t_2 \cos\alpha_3 + a^2}. \quad (10)$$

Performing the t_2 -integration we get

$$C_3^{\text{scalar}} = \int_0^{D_{23}} \frac{dt}{\sqrt{a^2 + t^2 \sin^2 \alpha_3}} \left(\arctan\left(\frac{D_{13} - t \cos\alpha_3}{\sqrt{a^2 + t^2 \sin^2 \alpha_3}}\right) + \arctan\left(\frac{t \cos\alpha_3}{\sqrt{a^2 + t^2 \sin^2 \alpha_3}}\right) \right). \quad (11)$$

To evaluate this integral in the limit of vanishing UV regulator a , we split into pieces and make suitable subtractions⁷ to arrive at ($\Theta(x)$ denotes the UnitStep function)

$$\begin{aligned} C_3^{\text{scalar}} &= \frac{\pi - \alpha_3}{\sin\alpha_3} \log \frac{2D_{23} \sin\alpha_3}{a} + \frac{\alpha_3 - \frac{\pi}{2}}{\sin\alpha_3} \log(\sin\alpha_3 + \sqrt{1 + \sin^2 \alpha_3}) \\ &+ \int_0^\infty \frac{dt}{\sqrt{1 + t^2 \sin^2 \alpha_3}} \left(\arctan\left(\frac{t \cos\alpha_3}{1 + t^2 \sin^2 \alpha_3}\right) + \left(\alpha_3 - \frac{\pi}{2}\right) \Theta(t - 1) \right) \\ &+ \frac{1}{\sin\alpha_3} \text{Im Li}_2\left(\frac{D_{23}}{D_{13}} e^{-i\alpha_3}\right) + \mathcal{O}(a \log a). \end{aligned} \quad (12)$$

Although not obviously, this is symmetrically in $D_{13} \leftrightarrow D_{23}$ as can be checked by using appropriate functional relations of the dilogarithm.

The edge contribution, e.g. for E_3^{scalar} is

$$\begin{aligned} E_3^{\text{scalar}} &= \frac{1}{2} \int_0^1 dt_1 \int_0^1 dt_2 \frac{1}{(t_1 - t_2)^2 + \frac{a^2}{D_{12}^2}} \\ &= \frac{\pi D_{12}}{2a} + \log \frac{a}{D_{12}} - 1 + \mathcal{O}(a^2). \end{aligned} \quad (13)$$

As mentioned above, the building blocks for (8) depend on both conformal and pure metrical invariants. Now we implement the closing to a triangle. Then, due to the sine law for standard triangles, we can replace the quotients of distances in the arguments of the dilogarithms by quotients of sines of the opposite angles. Then the only remaining dependence of the renormalised I from (8) on the distances D_{ij} has the form $-\gamma(\alpha_3)\log D_{23} - \gamma(\alpha_2)\log D_{12} - \gamma(\alpha_1)\log D_{13}$. To fit this to the structure required by (5), we add e.g. to the factor multiplying $-\gamma(\alpha_3)$ the term $\log \frac{D_{13}}{D_{12}}$ and

⁷Some details for the similar evaluation of the integrals in the generic case of a triangle with circular edges are presented in appendix B.

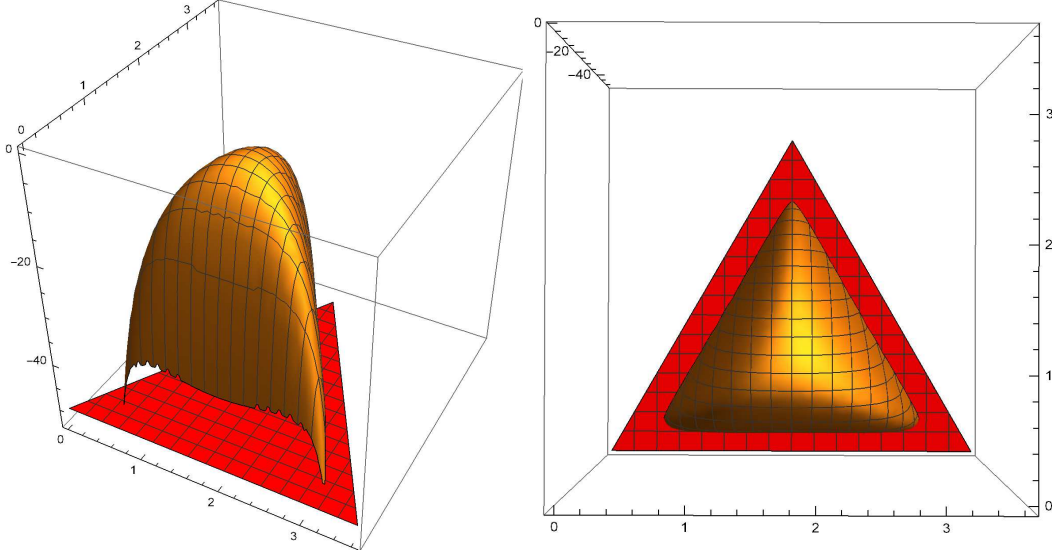


Figure 2: The remainder $\omega^{\text{st}}(\alpha_1, \alpha_2, \alpha_3)$ from two different perspectives. The angles are given by the distance to the edges of the red triangle in the (x, y) -plane. The plots exclude angles smaller than 0.3.

subtract it again after using the triangles sine law. This yields finally for the standard triangle remainder function of the Maldacena-Wilson loop with (9),(8),(7),(5),(3)

$$\begin{aligned}
\log \Omega^{\text{st}} &= \frac{g^2 C_F}{4\pi^2} \omega^{\text{st}} + \mathcal{O}(g^4) , \\
\omega^{\text{st}} &= \sum_{j=1}^3 \left(\gamma(\alpha_j) \log \frac{\sin \alpha_{j-1}}{2 \sin^2 \alpha_j} + \frac{1 + \cos \alpha_j}{\sin \alpha_j} \text{Im Li}_2 \left(\frac{\sin \alpha_{j+1}}{\sin \alpha_{j-1}} e^{-i\alpha_j} \right) \right. \\
&\quad + \gamma(\alpha_j) \frac{\alpha_j - \frac{\pi}{2}}{\alpha_j - \pi} \log(\sin \alpha_j + \sqrt{1 + \sin^2 \alpha_j}) \\
&\quad \left. + \int_0^\infty dt \frac{1 + \cos \alpha_j}{\sqrt{1 + t^2 \sin^2 \alpha_j}} \left(\arctan \left(\frac{t \cos \alpha_j}{\sqrt{1 + t^2 \sin^2 \alpha_j}} \right) + \left(\alpha_j - \frac{\pi}{2} \right) \Theta(t - 1) \right) \right) , \tag{14}
\end{aligned}$$

with the constraint $\sum_j \alpha_j = \pi$.⁸

To plot a numerical evaluation based on this formula in a manner symmetric in the α_j 's, we use the fact that for each point inside an equilateral triangle the sum of its distances to the edges is constant. For an edge length $2\pi/\sqrt{3}$ this sum is just equal to π . Then putting this equilateral triangle in the (x, y) -plane we have

$$\alpha_1 = y , \quad \alpha_2 = \frac{2\pi - \sqrt{3}x - y}{2} , \quad \alpha_3 = \frac{\sqrt{3}x - y}{2} . \tag{15}$$

The remainder $\omega^{\text{st}}(\alpha_1, \alpha_2, \alpha_3)$, via this formula as a function of x and y , is presented in fig.2. Its maximal value is -1.05373 , obtained for equal angles. Since ω^{st} diverges if one of the angles approaches zero, a certain neighbourhood of zero is excluded in the plots.

⁸Here and below we use the identification $j \pm 3 = j \text{ mod } 3$.

3 The generic triangle with circular edges

Denoting by δ_j the opening angle of the circular edge number j , i.e.

$$\sin \frac{\delta_j}{2} = \frac{D_{j-1,j+1}}{2R_j}, \quad (16)$$

we get by straightforward evaluation

$$E_j^{\text{scalar}} = \frac{\pi R_j \delta_j}{2a} + \log \frac{a}{D_{j-1,j+1}} - 1 + \mathcal{O}(a^2 \log a) \quad (17)$$

and

$$E_j^{\text{vector}} = E_j^{\text{scalar}} - \frac{\delta_j^2}{4} + \mathcal{O}(a^2). \quad (18)$$

Therefore the edge contribution to the supersymmetric Maldacena-Wilson loop is

$$\sum_j (E_j^{\text{scalar}} - E_j^{\text{vector}}) = \frac{1}{4} \sum_j \delta_j^2 + \mathcal{O}(a^2 \log a). \quad (19)$$

To evaluate the corner term C_3 , we map the corner number 3 with its two adjacent edges to a conformal frame where the corner is at infinity, see appendix A and [1]. The other corner terms are then given by cyclic permutations of the indices.

Let us start with the scalar contribution. Without regularisation ($a = 0$) the integrand of the scalar contribution to (4) is invariant under all conformal transformations. For $a > 0$ we get, after a shift to move corner 3 to the origin followed by an inversion and a dilatation to scale the distance between corners 1 and 2 to one,

$$\frac{|\dot{x}_1(t_1)| |\dot{x}_2(t_2)|}{(x_1 - x_2)^2 + a^2} = \frac{|\dot{y}_1(t_1)| |\dot{y}_2(t_2)|}{(y_1 - y_2)^2 + b_3^2 y_1^2 y_2^2}. \quad (20)$$

The abbreviation b_3 is defined by

$$b_3 = aD_3, \quad D_3 = \frac{D_{12}}{D_{13}D_{23}}. \quad (21)$$

Proceeding with

$$y_1(t_1) = Y_2 + t_1 e_2, \quad y_2(t_2) = Y_1 + t_2 e_1, \quad (22)$$

and Y_j and e_j defined as in appendix A,⁹ we get with (38),(39),(42)

$$(y_1(t_1) - y_2(t_2))^2 = 1 + t_1^2 + t_2^2 - 2t_1 t_2 \cos \alpha_3 + 2t_1 \cos \beta_1 + 2t_2 \cos \beta_2. \quad (23)$$

Taking the results of appendix B ($b \rightarrow b_3$, $\alpha \rightarrow \alpha_3$) we obtain from (21), (59),(77),(78)

$$C_3^{\text{scalar}} = \frac{\pi - \alpha_3}{\sin \alpha_3} \log \frac{D_{13} D_{23}}{D_{12}} + \frac{\pi - \alpha_3}{\sin \alpha_3} \log(2 \sin \alpha_3) + Q(\alpha_3, \beta_1, \beta_2). \quad (24)$$

⁹The use of this special form still requires some rotations, but these do not change the form of the r.h.s. of (20).

Now we turn to the more involved issue of the vector contribution . If the analogue of (20) would be true, with the nominators replaced by the scalar products of the tangents, C_3^{vector} would be given by C_3^{scalar} multiplied by $-\cos\alpha_3$. However, due to the violation of the invariance of even the unregularised integrand we get an additional contribution

$$C_3^{\text{vector}} = -\cos\alpha_3 C_3^{\text{scalar}} - A_3 . \quad (25)$$

Using a representation of the invariance breaking term as in [17] we calculate the A_j in appendix C and get from (92)

$$\sum_j A_j = \pi^2 + \sum_j (\beta_j^2 - (\pi - \alpha_j)^2 - \frac{1}{4}\delta_j^2) . \quad (26)$$

Collecting now (19),(24),(25),(26) for use in (5) and (8), we get with (6),(7) for the Maldacena-Wilson loop (Q as defined in appendix B, (78). For the planar case see also appendix D, (98),(100).)

$$\log \Omega = \frac{g^2 C_F}{4\pi^2} \omega + \mathcal{O}(g^4) , \quad (27)$$

$$\omega = \pi^2 + \sum_j ((1 + \cos\alpha_j) Q(\alpha_j, \beta_{j-1}, \beta_{j+1}) + \beta_j^2 - (\pi - \alpha_j)^2 - \gamma(\alpha_j)\log(2 \sin\alpha_j)) .$$

Furthermore, we note that the terms depending on the metrical invariants D_{ij} just organise to fit their appearance in (5). As expected, the dependence on the radii of the circular edges, encoded in the δ_j , cancels in the final result.

In a similar manner we find that for the pure gauge Wilson loop ω is replaced by

$$\begin{aligned} \omega^{\text{vec}} &= \pi^2 + 3 \\ &+ \sum_j (\cos\alpha_j Q(\alpha_j, \beta_{j-1}, \beta_{j+1}) + \beta_j^2 - (\pi - \alpha_j)^2 + (\pi - \alpha_j) \cot\alpha_j \log(2 \sin\alpha_j)) . \end{aligned} \quad (28)$$

To get some visual impression of the effect of torsion of the circular triangle, we look on the case, where all cusp angles α_j are equal and all torsion angles β_j are equal. Then we can generate in fig.3 a 3D-plot of the remainder ω as a function of two variables α and β . The region in the (α, β) -plane, allowed by geometry in 4D, is fixed by the discussion in appendix A, (48),(54),(57) as follows

$$-\frac{1}{2} \leq q \leq 1 \quad \text{with} \quad q = \frac{\cos\alpha + \cos^2\beta}{\sin^2\beta} . \quad (29)$$

$q = 1$ is reached for planar cases and $q = -\frac{1}{2}$ corresponds to cases, where the triangle is nonplanar, but can be embedded in a 3D subspace. The plot in fig.3 shows runaway behaviour in the vicinity of $(\alpha = 0, \beta = \frac{\pi}{2})$ and along the part of the red line with $\beta \geq \frac{\pi}{2}$. In the first case this is due to the obvious singularity related to the degeneration of the cusps to spikes with zero opening angle, see the fourth picture in fig.4 (compare also [13]). To understand the second case, we have to recall, that β measures the angle between the circular edges and the circumcircle. $q = 1$ implies a

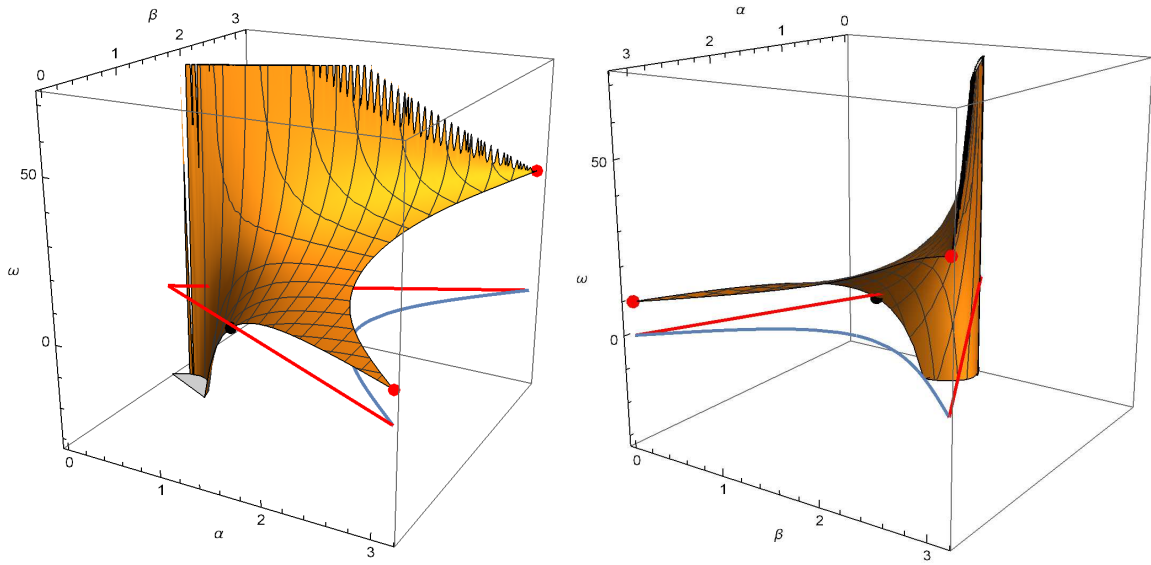


Figure 3: *The remainder $\omega(\alpha, \alpha, \alpha, \beta, \beta, \beta)$ from two different perspectives. The blue and red lines in the (α, β) -plane indicate the boundary of the geometrically allowed angles. The red line corresponds to planar triangles and the blue line to those embedded in a three-dimensional subspace. The black dot with $\alpha = \beta = \frac{\pi}{3}$ indicates the equilateral triangle with straight edges and the red dots mark the circle and the twice traversed circle, respectively.*

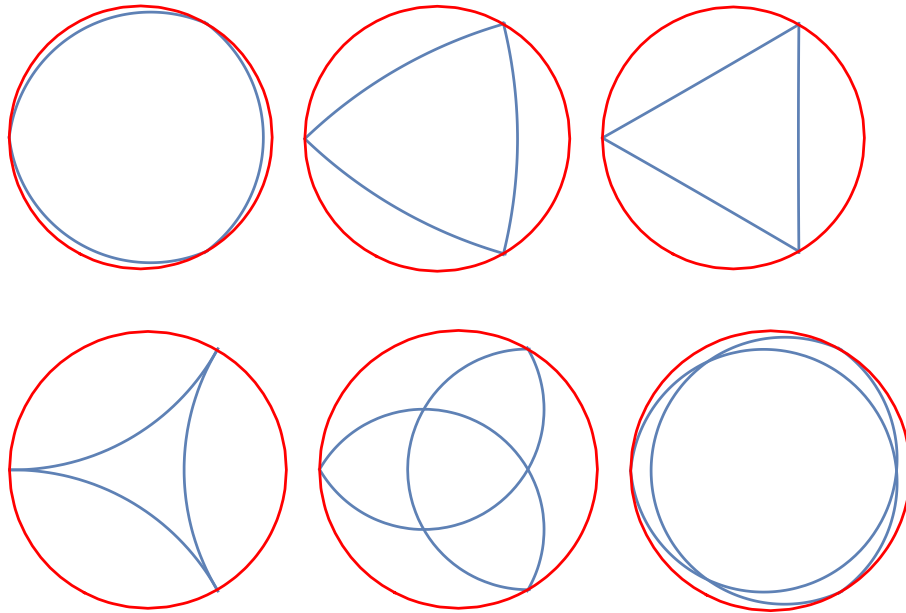


Figure 4: *The planar situation varying along the red line in fig.3 from a contour close to the simple circle to one close to the twice traversed circle. The circumcircle is shown in red.*

planar situation with all edges on the same side of the circumcircle. If then $\beta > \frac{\pi}{2}$, one

necessarily has self-intersections of the Wilson loop, see the last two pictures in fig.4 and the discussion at the end of appendix B.

Before closing this section, we still mention some consistency checks. At first let us consider the case $\beta = \frac{\pi - \alpha}{2}$. In the limit $\alpha \rightarrow \pi$ the corresponding contour becomes a circle (just the circumcircle of the triangle setting), and for both the supersymmetric as well as the pure gauge loop we expect the well-known result π^2 . Then the function Q diverges logarithmically. But due to its prefactor the expected result is obvious for the case of (27). To get the same result for (28) we can rely on

$$\lim_{\alpha \rightarrow \pi} \left(\cos \alpha Q\left(\alpha, \frac{\pi - \alpha}{2}, \frac{\pi - \alpha}{2}\right) + (\pi - \alpha) \cot \alpha \log(2 \sin \alpha) \right) = -1, \quad (30)$$

which has been checked numerically.

A similar limit is $\alpha \rightarrow \pi$ with $\beta = \frac{\pi + \alpha}{2}$. Then the contour approaches a twice traversed circle, see last picture in fig.4. Due to the degenerating self-intersections, the function Q diverges faster than a logarithm. Nevertheless, due to its prefactor in (27) one finds for the supersymmetric remainder the expected value $4\pi^2$. But for the pure vector remainder there remains a divergence.¹⁰

A third check comes from the limit, in which the generic circular triangle approaches a standard triangle with straight edges. First, as discussed in appendix A, the planar case, still with circular edges on the same side of the circumcircle, corresponds to $\alpha_j + \beta_{j-1} + \beta_{j+1} = \pi$, i.e.

$$\omega^{\text{planar}}(\alpha_j) = \omega\left(\alpha_j, \frac{\pi + \alpha_j - \alpha_{j-1} - \alpha_{j+1}}{2}\right). \quad (31)$$

Then ω^{planar} , calculated in this section by mapping parts of the contour to a conformal frame, has to be equal to ω^{st} , calculated without any mapping in the previous section, as soon as the sum of cusp angles is equal to π . This we have checked numerically over the full range of angles obeying this constraint.

A last comment concerns the generalisation to triangles where at the corners also a discontinuity in the coupling of the scalars is allowed. Let $\theta(t)$ in (2) be constant and equal to $\theta_{(j)}$ along edge number j , but

$$\cos \chi_j = \theta_{(j-1)} \cdot \theta_{(j+1)}. \quad (32)$$

This has no effect on the edge contributions and on the vector part of the corner terms in (8). Only the scalar corner terms pick up factors $\cos \chi_j$. This leads to a modification of the cusp anomalous dimension from (7) to [12]

$$\gamma(\alpha, \chi) = -(\pi - \alpha) \frac{\cos \chi + \cos \alpha}{\sin \alpha}. \quad (33)$$

Then use of this new form of γ has to be made in (27), and furthermore the prefactors $(1 + \cos \alpha_j)$ of the Q -terms become $(\cos \chi_j + \cos \alpha_j)$.

¹⁰This is not a disaster, since limits of the geometrical settings not necessarily have to commute with the renormalisation procedure.

The BPS case $\chi_j = \pi - \alpha_j$ simplifies to

$$\omega^{\text{BPS}} = \pi^2 + \sum_j (\beta_j^2 - (\pi - \alpha_j)^2) . \quad (34)$$

Furthermore, restricting ourselves to the planar case, and there e.g. to the same side situation with no selfcrossing $\alpha_j = \pi - \beta_{j-1} - \beta_{j+1}$, see (50), we get

$$\omega_{\text{planar}}^{\text{BPS}} = \frac{1}{4} \left(\sum_j \alpha_j - \pi \right) \left(5\pi - \sum_j \alpha_j \right) . \quad (35)$$

For all α_j equal to π we have the limiting case of a circle and get again the well-known result π^2 . The case $\sum_j \alpha_j = \pi$ covers standard triangles with straight edges and yields the result zero.

With the just discussed generalisation to cusps in the scalar coupling one can also specialise in a limit, where only scalar ladder diagrams survive [5], i.e. $g \rightarrow 0$, $N \rightarrow \infty$, $\chi_j \rightarrow i \infty$, with $\hat{g}_j^2 = \frac{g^2 C_F}{4\pi^2} \cos \chi_j$ fixed. Then one gets

$$\log \Omega|_{\text{CGL}} = \sum_j \hat{g}_j^2 (Q(\alpha_j, \beta_{j-1}, \beta_{j+1}) + \frac{\pi - \alpha_j}{\sin \alpha_j} \log(2 \sin \alpha_j)) + \mathcal{O}(\hat{g}_j^4) . \quad (36)$$

For planar triangles in [5] they have summed all orders. Our last formula, specialised to the planar case, corresponds then to the \hat{g}^2 order of their summation result.

4 Summary and conclusions

Our main result is the lowest order calculation of the remainder function of Wilson loops in $\mathcal{N} = 4$ SYM for triangles with circular edges, both for the supersymmetric (27) as well as for the pure vector case (28). It is given as a function of only conformal invariant parameters by standard functions and a convergent one-dimensional integral, suitable for immediate numerical evaluation. For the planar case a full representation in terms of standard functions has been found. In the limiting situations approaching a circle or a twice traversed circle we found agreement with the well-known results. Also the comparison of the respective limit with an independent calculation for the triangle with straight edges has given agreement.

We also commented on the obvious generalisation to cases where the coupling to the scalars is allowed to jump at the corners. In the related BPS case the dependence on the distances between the corners is absent and the remainder functions becomes a quadratic expression in the cusp and torsion angles, which in the planar situation simplifies even more to a quadratic expression in the sum of the cusp angles. It is zero for the standard triangles with straight edges. While in 2D these are the only cases with vanishing radiative corrections, in higher dimensions there is a whole variety with circular edges.

The appendix A extends the analysis of the conformal geometry of circular triangles started in [1]. We introduced for each building block, consisting out of a corner

and its two adjacent edges, an off-planarity parameter q_j . This allowed a formulation of the constraints imposed by the requirement of fitting these building blocks to a closed contour in a very compact and symmetric manner.

There are several interesting topics for further studies. One should look for a geometrical pattern behind the BPS loops with vanishing radiative corrections and its extension to higher orders. Combining the summation technique of [5] with our maps to conformal frames one should be able to generalise their results to non-planar circular triangles. To supplement our weak coupling results via AdS/CFT by a strong coupling analysis, one could try to relate the conformal parameters α_j, β_j to the local conformal invariant functions along smooth contours used in [14], [6] by promoting them to distributions. On pure geometrical level it would be nice to extend the closing conditions to higher circular polygons.

Acknowledgement:

I thank the Quantum Field and String Theory group at Humboldt University for kind virtual hospitality.

Appendix A: Conformal geometry of circular triangles

This appendix is an extension of appendix D in [1]. It handles the full 4D case and gives a nice symmetric form of the closing condition in 3D, which was lacking in that paper.

After a suitable translation, we can map the corner number 3 by a conformal inversion to infinity and scale, with a subsequent dilatation, the distance between the corners number 1 and 2 to one. Then by further using isometries we end up with a situation as follows. The images of the corners are $Y_1 = (0, 0, 0, 0)$, $Y_2 = (1, 0, 0, 0)$, $Y_3 = \infty$ and the circular edge number 3 is located in the $(1, 2)$ -plane and has negative 2-coordinates. The circumcircle is now the straight line along the 1-axis and the images of the edges number 1 and 2 are parts of straight lines through Y_2 and Y_1 , respectively. The unit vectors at Y_1 or Y_2 pointing in the direction of Y_3 along edges number 2 or 1 are

$$e_j = (\sin\psi_j \sin\vartheta_j \cos\varphi_j, \sin\psi_j \sin\vartheta_j \sin\varphi_j, \sin\psi_j \cos\vartheta_j, \cos\psi_j) . \quad (37)$$

Since at each corner the tangents to the circumcircle and the adjacent edges span at most a three-dimensional subspace, we can choose e.g. $\psi_2 = \frac{\pi}{2}$. This fixes our conformal frame, and the following 6 conformal invariants characterise a circular

triangle in 4D

$$\psi_1, \vartheta_1, \vartheta_2, \varphi_1, \varphi_2, \quad \text{and} \quad \beta_3 .$$

For an illustration of its 3D projection see figure 4 in [1]. The three cusp and the two remaining torsion angles are then given by

$$\cos\beta_1 = \sin\vartheta_2 \cos\varphi_2 , \quad (38)$$

$$\cos\beta_2 = -\sin\psi_1 \sin\vartheta_1 \cos\varphi_1 . \quad (39)$$

$$\cos\alpha_1 = \sin\psi_1 \sin\vartheta_1 \cos(\beta_3 + \varphi_1) , \quad (40)$$

$$\cos\alpha_2 = -\sin\vartheta_2 \cos(\beta_3 - \varphi_2) , \quad (41)$$

$$\begin{aligned} \cos\alpha_3 &= \sin\psi_1 (\cos\vartheta_1 \cos\vartheta_2 + \sin\vartheta_1 \sin\vartheta_2 \cos(\varphi_1 - \varphi_2)) \\ &= \sin\psi_1 (\cos\vartheta_1 \cos\vartheta_2 + \sin\vartheta_1 \sin\vartheta_2 \sin\varphi_1 \sin\varphi_2) - \cos\beta_1 \cos\beta_2 . \end{aligned} \quad (42)$$

Using (39) and (40) to express ϑ_1, φ_1 in terms of $\alpha_1, \beta_2, \beta_3$ we get

$$\sin^2\psi_1 \sin^2\vartheta_1 = \frac{\cos^2\alpha_1 + \cos^2\beta_2 + 2\cos\alpha_1 \cos\beta_2 \cos\beta_3}{\sin^2\beta_3} , \quad (43)$$

$$\cos^2\varphi_1 = \frac{\cos^2\beta_2 \sin^2\beta_3}{\cos^2\alpha_1 + \cos^2\beta_2 + 2\cos\alpha_1 \cos\beta_2 \cos\beta_3} , \quad (44)$$

and similarly with (38) and (41)

$$\sin^2\vartheta_2 = \frac{\cos^2\alpha_2 + \cos^2\beta_1 + 2\cos\alpha_2 \cos\beta_1 \cos\beta_3}{\sin^2\beta_3} , \quad (45)$$

$$\cos^2\varphi_2 = \frac{\cos^2\beta_1 \sin^2\beta_3}{\cos^2\alpha_2 + \cos^2\beta_1 + 2\cos\alpha_2 \cos\beta_1 \cos\beta_3} . \quad (46)$$

Inserting this in (42) we get¹¹

$$\sin\psi_1 \cos\vartheta_1 \cos\vartheta_2 = (q_3 - q_1 q_2) \sin\beta_1 \sin\beta_2 \quad (47)$$

with

$$q_j = \frac{\cos\alpha_j + \cos\beta_{j+1} \cos\beta_{j-1}}{\sin\beta_{j+1} \sin\beta_{j-1}} . \quad (48)$$

After squaring (47) and a little bit more algebra we arrive at

$$1 + 2q_1 q_2 q_3 - q_1^2 - q_2^2 - q_3^2 = \frac{\cos^2\psi_1 \cos^2\vartheta_2}{\sin^2\beta_1 \sin^2\beta_2} . \quad (49)$$

Each q_j is a parameter characterising a corner of the triangle with its two adjacent circular edges. For a planar circular triangle, or one which is completely located at a sphere, one has, e.g. for q_3 , either

$$\alpha_3 = |\pi - (\beta_1 + \beta_2)|, \quad \text{or} \quad \alpha_3 = \pi - |\beta_1 - \beta_2| . \quad (50)$$

¹¹Taking into account, that all angles except the φ 's are in $(0, \pi)$ and that for $\varphi_j \in (0, 2\pi)$ the signs of $\sin\varphi_j$ are correlated to that of q_j by $\text{sign } q_j = -\text{sign } \sin\varphi_j$ for *both* $j = 1$ and $j = 2$.

This implies

$$q_j = \pm 1 \quad (\text{planar case}) , \quad (51)$$

depending on whether the two adjacent edges are on the same or opposite sides of the circumcircle.¹²

In the generic 4D situation we have,

$$\cos\alpha_3 = -\cos\beta_1\cos\beta_2 + \sin\beta_1\sin\beta_2 \vec{u}_1\vec{u}_2 , \quad (52)$$

with \vec{u}_1 and \vec{u}_2 three-dimensional unit vectors describing at corner number 3 the projection of the tangents to the edges on the subspace perpendicular to the tangent to the circumcircle. Hence instead of (50) one gets,

$$|\pi - (\beta_1 + \beta_2)| \leq \alpha_3 \leq \pi - |\beta_1 - \beta_2| \quad (53)$$

and cyclic permutations for the other two corners. As a consequence of the last inequalities we get

$$|q_j| \leq 1 . \quad (54)$$

Hence the q_j 's are some kind of off-planarity parameters for their corresponding corners with their two adjacent edges. Varying a certain q_j from 1 to -1 one interpolates between the planar same side situation and the planar opposite side situation via additional dimensions.

Comparing q_j with a standard measure for off-planarity, the three-dimensional Gram determinant G_j of the tangent vectors at X_j on the circumcircle and on the two neighbouring edges, we find

$$G_j = \sin^2\beta_{j-1}\sin^2\beta_{j+1}(1 - q_j^2) . \quad (55)$$

We now come back to (49). With (38) and (39) one can bring its r.h.s. in the form

$$\frac{\cos^2\vartheta_2}{\cos^2\vartheta_2 + \sin^2\vartheta_2\sin^2\varphi_2} \cdot \frac{\cos^2\psi_1}{\cos^2\psi_1 + \sin^2\psi_1(\cos^2\vartheta_1 + \sin^2\vartheta_1\sin^2\varphi_1)} .$$

Obviously it is a positive number between zero and one and it depends on ψ_1 , a parameter not correlated with the q_j 's, i.e.

$$1 + 2 q_1 q_2 q_3 - q_1^2 - q_2^2 - q_3^2 \in (0, 1) . \quad (56)$$

The off-planarity parameters q_j characterise the building blocks, consisting of corners with adjacent edges. ψ_1 parameterises the torsion between the three-dimensional subspaces spanned by two of these building blocks.

Then altogether we can state: The off-planarity parameters q_j for the three building blocks are by their intrinsic geometry constrained by (54). If one wants to combine them to a closed triangle in 4D, they have in addition to obey the inequality¹³¹⁴

$$1 + 2 q_1 q_2 q_3 - q_1^2 - q_2^2 - q_3^2 \geq 0 . \quad (57)$$

¹²Note that in the planar case with circular edges on the same side of the circumcircle for $\beta_1 + \beta_2 > \pi$ one has to handle an additional UV divergence due to a crossing of the edges.

¹³The other bound from (56) is automatically realised due to (54).

¹⁴As an interesting side remark, note that the condition (57) after $q_j = 2u_j - 1$ coincides with that for the allowed region of the three cross ratios u_1, u_2, u_3 , describing the conformal geometry of null hexagons [15, 16].

In 3D, i.e. $\psi_1 = \frac{\pi}{2}$, the inequality has to be saturated. This then is related to the reduction of the number of conformal invariants from 6 to 5. In 2D, due to (51), remains the condition $q_1 q_2 q_3 = 1$. It simply states, that only zero or two corners with opposite side edges are allowed for closing.

The points in q -space, constrained by (54) and (57) are illustrated in the left of fig.5. For a circular triangle in 4D one is restricted to the interior of the rounded tetraeder, in 3D to its boundary and in 2D to one of its 4 corners.

For a fixed value of α_3 , the region allowed by (53) is a rectangle within the square $\beta_1, \beta_2 \in (0, \pi)$, placed symmetrically around the diagonals

$$\pi - \alpha \leq \beta_1 + \beta_2 \leq \pi + \alpha, \quad |\beta_1 - \beta_2| \leq \pi - \alpha. \quad (58)$$

Since $\beta_1 + \beta_2$ on its upper bound is larger than π this corresponds to the same side planar case with crossing edges. On the lower bound there is no crossing.

The function $q_3(\beta_1, \beta_2, \alpha_3)$ is visualised in the right part of fig.5. The boundaries of the rectangles correspond to the planar situation. Along the lower and upper boundary for $\beta_1 + \beta_2$ one has $q_3 = 1$ and on the lower and upper boundary for $\beta_1 - \beta_2$ one has $q_3 = -1$.¹⁵

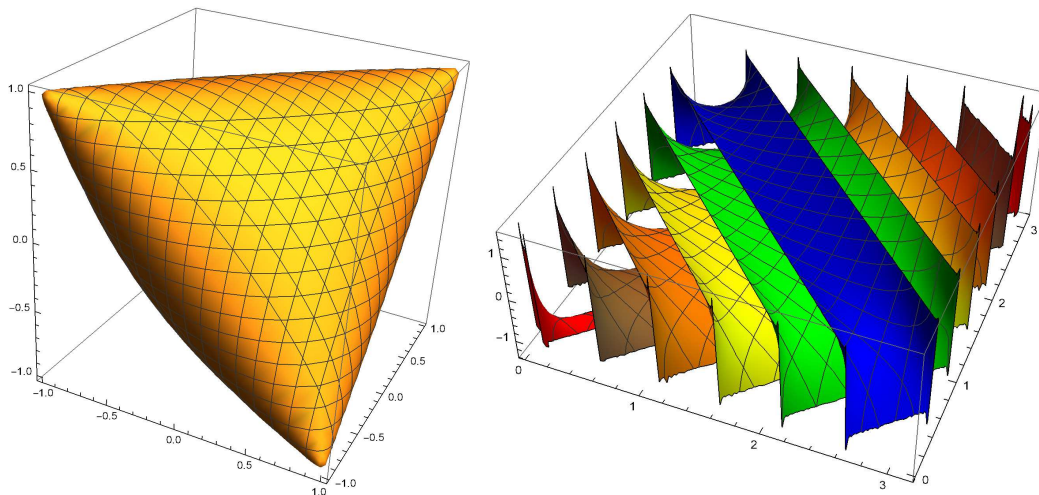


Figure 5: *Left: Locus of points (q_1, q_2, q_3) , allowed by the constraints (57) and (54). Right: q_3 as a function of β_1 and β_2 for various values of α_3 . Shown are equidistant steps for α_3 , starting from 0.5 in blue up to 3 in red.*

¹⁵Since the limit for q_3 at the corners depends on the direction of its approach, the numerical evaluation near the corners becomes unstable. This explains the apparent spikes at the corners in fig.5.

Appendix B: Integral for scalar corner term

Here we study the $b \rightarrow 0$ limit of

$$J(\alpha, \beta_1, \beta_2, b) = \int_0^\infty \frac{dt_1 dt_2}{1 + t_1^2 + t_2^2 - 2t_1 t_2 \cos\alpha + 2t_1 \cos\beta_1 + 2t_2 \cos\beta_2 + b^2 f(t_1, t_2)}, \quad (59)$$

where $f(t_1, t_2)$ has the structure

$$f(t_1, t_2) = t_1^2 t_2^2 + g(t_1, t_2), \quad (60)$$

with $g(t_1, t_2)$ a polynomial in t_1 and t_2 whose overall degree is only three. It arises if (22) is inserted in (20).

We are interested in the logarithmic divergence and the finite term for $b \rightarrow 0$ and argue at first, that for this purpose $g(t_1, t_2)$ can be neglected. Denoting the denominator in(59) without the $b^2 f$ -term as D we can write

$$J = \int_0^\infty \frac{dt_1 dt_2}{D + b^2 t_1^2 t_2^2} + \int_0^\infty \frac{dt_1 dt_2}{D + b^2 t_1^2 t_2^2} \left(\left(1 + \frac{b^2 g(t_1, t_2)}{D + b^2 t_1^2 t_2^2} \right)^{-1} - 1 \right). \quad (61)$$

The maximum of $\left| \frac{b^2 g(t_1, t_2)}{D + b^2 t_1^2 t_2^2} \right|$ in the whole integration region is of order $\mathcal{O}(b)$, hence we can conclude that the second integral in (61) is of order $\mathcal{O}(b \log b)$.

Then, after performing in the first integral the t_2 -integration we get ¹⁶

$$J(\alpha, \beta_1, \beta_2, b) = \int_0^\infty \frac{dt}{\sqrt{S(t) + b^2 t^4}} \left(\frac{\pi}{2} - \arctan\left(\frac{\cos\beta_2 - t \cos\alpha}{\sqrt{S(t) + b^2 t^4}} \right) \right) + \mathcal{O}(b \log b), \quad (62)$$

with

$$S(t) = t^2 \sin^2 \alpha + 2t(\cos\beta_1 + \cos\beta_2 \cos\alpha) + \sin^2 \beta_2. \quad (63)$$

For $b = 0$, the integrand behaves for $t \rightarrow \infty$ as $(\pi - \alpha)/(t \sin\alpha)$. Trivially, this is the source for a logarithmic divergence. A little bit more effort is needed to extract also the not divergent, but finite part in the limit $b \rightarrow 0$.

To this end we split the integral into pieces in a sequence of steps. First into integrals from zero to one and from one to infinity. In the first piece b can be put to zero under the integral. Hence

$$J(\alpha, \beta_1, \beta_2, b) = J_0(\alpha, \beta_1, \beta_2) + J_1(\alpha, \beta_1, \beta_2, b) + \mathcal{O}(b \log b) + \mathcal{O}(b^2), \quad (64)$$

with

$$J_0(\alpha, \beta_1, \beta_2) = \int_0^1 \frac{dt}{\sqrt{S(t)}} \left(\frac{\pi}{2} - \arctan\left(\frac{\cos\beta_2 - t \cos\alpha}{\sqrt{S(t)}} \right) \right), \quad (65)$$

$$J_1(\alpha, \beta_1, \beta_2, b) = \int_1^\infty \frac{dt}{\sqrt{S(t) + b^2 t^4}} \left(\frac{\pi}{2} - \arctan\left(\frac{\cos\beta_2 - t \cos\alpha}{\sqrt{S(t) + b^2 t^4}} \right) \right). \quad (66)$$

¹⁶Strictly speaking the t_2 -integration yields the expression, where $b^2(t^4 + 2t^3 \cos\beta_1 + t^2)$ stands instead of only $b^2 t^4$. But repeating the argumentation from just above, the error is again vanishing for $b \rightarrow 0$.

For the second split we concentrate on the first factor of the integrand in J_1 , write it as $1/\sqrt{t^2\sin^2\alpha + b^2t^4} + (1/\sqrt{S(t) + b^2t^4} - 1/\sqrt{t^2\sin^2\alpha + b^2t^4})$ and send b to zero in the subtracted term. Then we get

$$J_1(\alpha, \beta_1, \beta_2, b) = J_{11}(\alpha, \beta_1, \beta_2, b) + J_{10}(\alpha, \beta_1, \beta_2) + \mathcal{O}(b^2), \quad (67)$$

$$J_{11}(\alpha, \beta_1, \beta_2, b) = \int_1^\infty \frac{dt}{\sqrt{t^2\sin^2\alpha + b^2t^4}} \left(\frac{\pi}{2} - \arctan\left(\frac{\cos\beta_2 - t\cos\alpha}{\sqrt{S(t) + b^2t^4}}\right) \right), \quad (68)$$

$$J_{10}(\alpha, \beta_1, \beta_2) = \int_1^\infty dt \left(\frac{1}{\sqrt{S(t)}} - \frac{1}{t\sin\alpha} \right) \left(\frac{\pi}{2} - \arctan\left(\frac{\cos\beta_2 - t\cos\alpha}{\sqrt{S(t)}}\right) \right). \quad (69)$$

So far J_0 and J_{10} are finite and J_{11} still divergent for $b \rightarrow 0$. The last splitting now concerns J_{11} . Keeping in mind $\arctan(-\cot\alpha) = \alpha - \pi/2$, we write

$$J_{11}(\alpha, \beta_1, \beta_2, b) = J_{11}^{(1)}(\alpha, b) + J_{11}^{(2)}(\alpha, \beta_1, \beta_2) + J_{11}^{(3)}(\alpha, \beta_1, \beta_2, b) + \mathcal{O}(b^2), \quad (70)$$

$$J_{11}^{(1)}(\alpha, b) = (\pi - \alpha) \int_1^\infty \frac{dt}{\sqrt{t^2\sin^2\alpha + b^2t^4}}, \quad (71)$$

$$J_{11}^{(2)}(\alpha, \beta_1, \beta_2) = \int_1^\infty \frac{dt}{t\sin\alpha} \left(\alpha - \frac{\pi}{2} - \arctan\left(\frac{\cos\beta_2 - t\cos\alpha}{\sqrt{S(t)}}\right) \right), \quad (72)$$

$$J_{11}^{(3)}(\alpha, \beta_1, \beta_2, b) = \int_1^\infty \frac{dt}{\sqrt{t^2\sin^2\alpha + b^2t^4}} \left(\arctan\left(\frac{\cos\beta_2 - t\cos\alpha}{\sqrt{S(t)}}\right) - \arctan\left(\frac{\cos\beta_2 - t\cos\alpha}{\sqrt{S(t) + b^2t^4}}\right) \right). \quad (73)$$

$J_{11}^{(1)}$ is a standard integral and expressed as

$$J_{11}^{(1)}(\alpha, b) = \frac{\pi - \alpha}{\sin\alpha} \log \frac{2\sin\alpha}{b} + \mathcal{O}(b^2). \quad (74)$$

To get under control the $b \rightarrow 0$ limit of $J_{11}^{(3)}$, we substitute the integration variable via $t = 1/(bu)$ and arrive with (63) at

$$J_{11}^{(3)}(\alpha, \beta_1, \beta_2, b) = \int_0^{1/b} \frac{du}{\sqrt{1 + u^2\sin^2\alpha}} \left(\arctan\left(\frac{bu\cos\beta_2 - \cos\alpha}{\sqrt{\sin^2\alpha + 2bu(\cos\beta_1 + \cos\beta_2\cos\alpha) + b^2u^2\sin^2\beta_2}}\right) - \arctan\left(\frac{bu\cos\beta_2 - \cos\alpha}{\sqrt{\sin^2\alpha + 2bu(\cos\beta_1 + \cos\beta_2\cos\alpha) + b^2u^2\sin^2\beta_2 + 1/u^2}}\right) \right) \quad (75)$$

Now we see that the limit $b \rightarrow 0$ exists and find

$$J_{11}^{(3)}(\alpha, \beta_1, \beta_2, b) = \int_0^\infty \frac{du}{\sqrt{1 + u^2\sin^2\alpha}} \left(\alpha - \frac{\pi}{2} + \arctan\left(\frac{u\cos\alpha}{\sqrt{1 + u^2\sin^2\alpha}}\right) \right) + \mathcal{O}(b). \quad (76)$$

Finally, collecting (64),(65),(67),(69)(70),(71),(72),(76) we get

$$J(\alpha, \beta_1, \beta_2, b) = \mathcal{O}(b \log b) + \mathcal{O}(b) + \frac{\pi - \alpha}{\sin \alpha} \log \frac{2 \sin \alpha}{b} + Q(\alpha, \beta_1, \beta_2), \quad (77)$$

$$\begin{aligned} Q(\alpha, \beta_1, \beta_2) &= \int_0^\infty \frac{dt}{\sqrt{1+t^2 \sin^2 \alpha}} \left(\alpha - \frac{\pi}{2} + \arctan \left(\frac{t \cos \alpha}{\sqrt{1+t^2 \sin^2 \alpha}} \right) \right) \\ &+ \int_0^1 \frac{dt}{\sqrt{S(t)}} \left(\frac{\pi}{2} - \arctan \left(\frac{\cos \beta_2 - t \cos \alpha}{\sqrt{S(t)}} \right) \right) \\ &+ \int_1^\infty dt \left(\frac{\alpha - \pi}{t \sin \alpha} + \frac{1}{\sqrt{S(t)}} \left(\frac{\pi}{2} - \arctan \left(\frac{\cos \beta_2 - t \cos \alpha}{\sqrt{S(t)}} \right) \right) \right), \end{aligned} \quad (78)$$

with S as function of $\alpha, \beta_1, \beta_2, t$ defined in (63).

For the first integral in (78), let us call it $Q_0(\alpha)$, we found a representation in terms of log's and dilog's

$$Q_0 = \frac{1}{\sin \alpha} \left(\left(\alpha - \pi \Theta \left(\alpha - \frac{\pi}{2} \right) \right) \log \sin \alpha - \frac{1}{2} \text{Im Li}_2(-e^{2i\alpha}) + \text{Im Li}_2 \left(\frac{1 - e^{2i\alpha}}{2} \right) \right). \quad (79)$$

It remains an interesting open question, whether there is a similar representation also for the other two integrals, which depend besides on α also on the two torsion angles. In the simpler planar case $S(t)$ is a pure square, and we present such a representation of the corresponding full Q in appendix D, see (98),(100).

For the case C_3 in the main text take $\alpha = \alpha_3$, $b = \frac{D_{12}}{D_{23}D_{13}}a$ and cyclic permutations for the other C_j .

Our function $Q(\alpha, \beta_1, \beta_2)$ was constructed as the finite part after subtracting the UV divergent terms due to the cusp at the corner under consideration. As stated in the previous appendix, along the upper bound of $\beta_1 + \beta_2$ one has a planar situation with crossing edges. This so far neglected additional UV divergence has to show up as a divergence of Q .

To illustrate this issue, let us start with the observation, that the only potential source for a divergence of Q could be related to zeros of the quadratic polynomial $S(t)$. Inside (58) they are either complex or negative, hence outside the integration region for t . On the lower boundary of $\beta_1 + \beta_2$ (same side planar case without crossing) one finds a double zero at negative values of t , i.e. no divergence. A double zero at positive t -values on gets on the upper boundary of $\beta_1 + \beta_2$ and on both boundaries of $\beta_1 - \beta_2$. At a zero t_0 of $S(t)$ the arctan in the second and third integral in (78) approaches $\pm \frac{\pi}{2}$, depending on the sign of $\cos \beta_2 - t_0 \cos \alpha$. It turns out to be positive on both boundaries of $\beta_1 - \beta_2$, the opposite side planar cases, and negative on the upper boundary of $\beta_1 + \beta_2$. Therefore, Q is only divergent along the upper boundary of $\beta_1 + \beta_2$.

We present some plots of Q in fig.6, with a small neighbourhood of the upper bound of $\beta_1 + \beta_2$ excluded. A hasty view might suggest the impression that the shown bands would be flat. To avoid this mistake, we show cuts along the lines of constant $\beta_1 + \beta_2$ at the lower and very near to the upper end in fig.7.

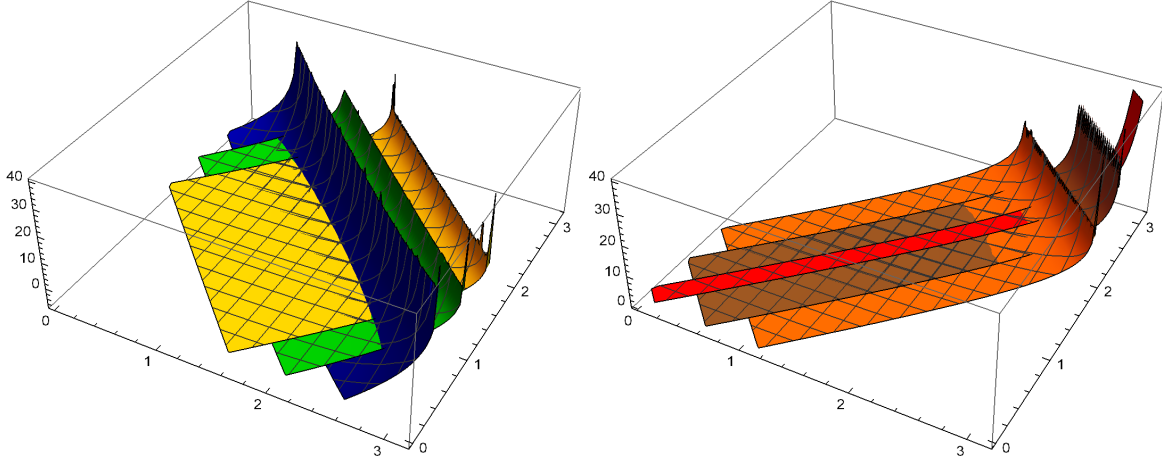


Figure 6: The function $Q(\alpha, \beta_1, \beta_2)$ in dependence on β_1, β_2 for different values of α . On the left in blue, green, yellow for $\alpha = 0.5, 1.0, 1.5$ and on the right in orange, brown and red for $\alpha = 2.0, 2.5, 3.0$.

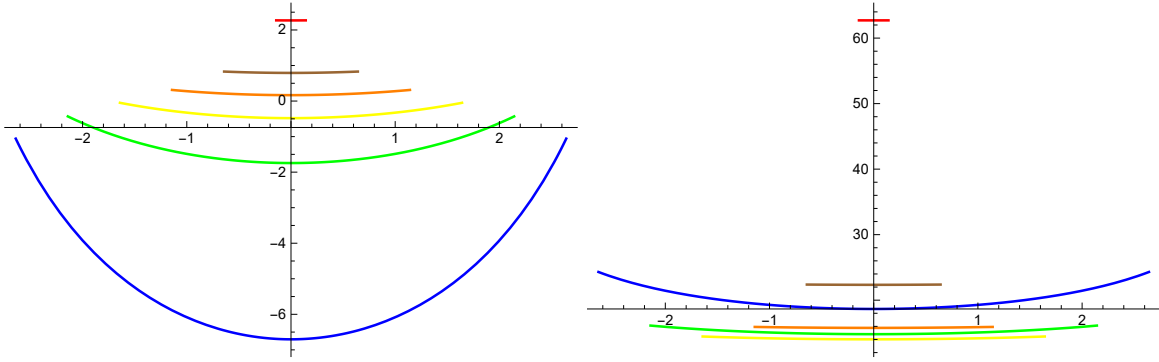


Figure 7: Q as a function of $\beta_1 - \beta_2$. On the left at the lower boundary of $\beta_1 + \beta_2$ and on the right at a distance 0.02 from the upper boundary of $\beta_1 + \beta_2$. The corresponding values of α are encoded in colours as in fig.6.

Appendix C: Correction term for map to conformal frame

In this appendix we sketch the calculation of the correction terms A_j in (25), generated by the mapping to the respective conformal frame. We write the formulas for A_3 , the other cases one gets by cyclic permutation of indices.

Under a conformal inversion $x = \frac{w}{w^2}$ one has

$$\begin{aligned} (x_1 - x_2)^2 &= \frac{1}{w_1^2 w_2^2} (w_1 - w_2)^2, \\ \dot{x}_j^\mu &= \frac{1}{w_j^2} I^{\mu\nu}(w_j) \dot{w}_j^\nu, \quad \text{with} \quad I^{\mu\nu}(w) = \delta^{\mu\nu} - 2 \frac{w^\mu w^\nu}{w^2}. \end{aligned} \quad (80)$$

This guarantees the invariance of the unregularised scalar contribution used in (20), but implies for the vector contribution

$$\frac{\dot{x}_1 \dot{x}_2}{(x_1 - x_2)^2} = \frac{I^{\mu\lambda}(w_1) I^{\nu\lambda}(w_2) \dot{w}_1^\mu \dot{w}_2^\nu}{(w_1 - w_2)^2}, \quad (81)$$

which leads to [17]

$$\begin{aligned} \frac{\dot{x}_1 \dot{x}_2}{(x_1 - x_2)^2} &= \frac{\dot{w}_1 \dot{w}_2}{(w_1 - w_2)^2} + \dot{w}_1^\mu \dot{w}_2^\nu \left(\frac{w_2^\nu}{w_2^2} \partial_1^\mu \log(w_1 - w_2)^2 \right. \\ &\quad \left. + \frac{w_1^\mu}{w_1^2} \partial_2^\nu \log(w_1 - w_2)^2 - \frac{1}{2} \partial_1^\mu \log w_1^2 \partial_2^\nu \log w_2^2 \right). \end{aligned} \quad (82)$$

The derivative structure of the correction term leads to the invariance of the related integral for closed contours not passing the origin and to the anomaly discussed in [17], if the origin is on the contour. But for our corner building block we have to handle an open (part of) contour.

At the beginning of appendix A we have described a stepwise map of a corner building block, e.g. corner number 3 with adjacent edges, to its conformal frame. Among these steps only the second one, an inversion, contributes to A_3 . Taking into account the preceding translation to move corner number 3 to the origin, the images of the corners after the inversion are

$$W_1 = \frac{X_1 - X_3}{D_{13}^2}, \quad W_2 = \frac{X_2 - X_3}{D_{23}^2}, \quad W_3 = \infty. \quad (83)$$

The images of the edges in w -space are then parameterised by

$$w_1(t_1) = W_2 + t_1 n_2, \quad w_2(t_2) = W_1 + t_2 n_1, \quad (84)$$

and in the sense of a universal contour parameter along the whole corner contribution we have

$$\dot{w}_1 \dot{w}_2 = -n_1 n_2 = -\cos \alpha_3. \quad (85)$$

The derivative structure of (83) allows to perform trivial integrations, and we get with a preliminary IR cutoff Λ

$$\begin{aligned} A_3 &= \int_0^\Lambda \frac{dt (W_1 n_1 + t)}{t^2 + 2tW_1 n_1 + W_1^2} (\log(W_2 - W_1 + \Lambda n_2 - t n_1)^2 - \log(W_2 - W_1 - t n_1)^2) \\ &\quad + (1 \leftrightarrow 2) - \frac{1}{2} (\log(W_1 + \Lambda n_1)^2 - \log(W_1^2)) (\log(W_2 + \Lambda n_2)^2 - \log(W_2^2)). \end{aligned} \quad (86)$$

Let us call the integral in the first line of the formula above G_{13} (integration between corner 1 and corner 3) and expand the last term for large Λ we get

$$A_3 = G_{13} + G_{23} - 2(\log \Lambda)^2 + \log \Lambda (\log W_1^2 + \log W_2^2) - \frac{\log W_1^2 \log W_2^2}{2} + \mathcal{O}\left(\frac{\log \Lambda}{\Lambda}\right). \quad (87)$$

Introducing the indefinite integral

$$H(K, L, M, N, x) = \int \frac{x + K}{x^2 + 2Kx + L} \log(x^2 + 2Mx + N) dx, \quad (88)$$

we get

$$G_{13} = H(K, L, \hat{M}, \hat{N}, \Lambda) + H(K, L, \tilde{M}, \tilde{N}, \Lambda) - H(K, L, \hat{M}, \hat{N}, 0) - H(K, L, \tilde{M}, \tilde{N}, 0), \quad (89)$$

with

$$\begin{aligned} K &= W_1 n_1, \quad L = W_1^2, \quad \hat{M} = (W_1 - W_2) n_1 - \Lambda \cos \alpha_3, \\ \hat{N} &= (W_2 - W_1)^2 + 2\Lambda(W_2 - W_1) n_2 + \Lambda^2, \quad \tilde{M} = (W_1 - W_2) n_1, \quad \tilde{N} = (W_2 - W_1)^2. \end{aligned} \quad (90)$$

Using the invariance of angles under the mapping and that the image of the circumcircle is given by the straight line passing W_1 and W_2 , we can express the just introduced constants via (83) in terms of parameters of the original setting (δ_j defined in (16), D_3 in (21))

$$\begin{aligned} K &= \frac{1}{D_{13}} \cos \frac{\delta_2}{2}, \quad L = \frac{1}{D_{13}^2}, \quad \hat{M} = D_3 \cos \beta_2 - \Lambda \cos \alpha_3, \\ \hat{N} &= D_3^2 + 2\Lambda D_3 \cos \beta_1 + \Lambda^2, \quad \tilde{M} = D_3 \cos \beta_2, \quad \tilde{N} = D_3^2. \end{aligned} \quad (91)$$

As defined in (88) H , is given by a sum of logarithms and dilogarithms, in which some of the terms have complex arguments. Neither for G_{13} , nor for the combination $G_{13} + G_{23}$, needed for A_3 in (87), we could eliminate the dilogarithms in favour of logarithms via their standard functional relations. However, one can reach this goal for the sum of all G_{ij} terms appearing in the sum $A_1 + A_2 + A_3$. Then after a massage of the many remaining logarithms, careful handling of phases of complex terms and expanding for large IR cutoff Λ we find cancellation of the IR divergent terms and finally a very compact expression for the remaining finite contribution

$$A_1 + A_2 + A_3 = \pi^2 + \sum_j (\beta_j^2 - (\pi - \alpha_j)^2 - \frac{1}{4} \delta_j^2). \quad (92)$$

Appendix D: Function Q in the planar case in terms of standard functions

In this appendix we specialise in the planar case and sketch the representation of the whole function Q , given in (78) by three convergent one-dimensional integrals, in terms of standard functions.

The function $S(t)$, defined by (63), can be rewritten as

$$S(t) = \sin^2 \alpha \left(\left(t + \frac{\cos \beta_1 + \cos \beta_2 \cos \alpha}{\sin^2 \alpha} \right)^2 + \frac{(1 - q^2) \sin^2 \beta_1 \sin^2 \beta_2}{\sin^4 \alpha} \right), \quad (93)$$

with the off-planarity parameter q defined according to (48). In the planar case we have $|q| = 1$ and S becomes a pure square. Furthermore, the three angles α, β_1, β_2 are no longer independent. With (50) we get

$$S(t)|_{\text{planar}} = (t \sin\beta + \sin\beta_2)^2, \quad \text{with } \beta = \beta_1 + \beta_2 \text{ or } \beta = |\beta_1 - \beta_2| \quad (94)$$

in the cases where the edges are on the same or opposite side of the circumcircle, respectively.

Then the only nontrivial integrations, needed in the second and third row of (78) are of the type

$$\begin{aligned} U(t_1, t_2) &= \int_{t_1}^{t_2} \frac{dt}{t \sin\beta + \sin\beta_2} \arctan\left(\frac{\cos\beta_2 + t \cos\beta}{\sin\beta_2 + t \sin\beta}\right) \\ &= \frac{1}{\sin\beta} \int_{x(t_2)}^{x(t_1)} \frac{dx}{x} \arctan(\cot\beta + x), \quad \text{with } x(t_j) = \frac{\sin(\beta - \beta_2)}{t_j \sin^2\beta + \sin\beta \sin\beta_2}. \end{aligned} \quad (95)$$

The related indefinite integral is

$$\int \frac{dx}{x} \arctan(A+x) = \text{Im} \left\{ \log\left(-\frac{x}{A-i}\right) \log(1+i(A+x)) - \text{Li}_2\left(\frac{x+A+i}{A+i}\right) \right\}. \quad (96)$$

Let us now remember, that due to their geometrical meaning $\beta_1, \beta_2 \in (0, \pi)$. In the same side case we restrict ourselves to $\beta_1 + \beta_2 < \pi$, because otherwise the two edges intersect, causing divergences. In the opposite side case one always has $\beta < \pi$ and we assume in addition w.l.o.g. $\beta_2 > \beta_1$. Therefore the boundary values needed for the x -integrations in (96) are positive in the same side case and negative in the opposite side case. With this in mind and taking into account (79), we finally get for

$$\begin{aligned} Q_{\text{same}}^{\text{planar}}(\beta_1, \beta_2) &= Q(\pi - (\beta_1 + \beta_2), \beta_1, \beta_2), \quad \beta_1 + \beta_2 < \pi \\ Q_{\text{oppo}}^{\text{planar}}(\beta_1, \beta_2) &= Q(\pi - |\beta_1 - \beta_2|, \beta_1, \beta_2), \end{aligned} \quad (97)$$

the following expressions in terms of standard functions¹⁷

$$\begin{aligned} Q_{\text{same}}^{\text{planar}}(\beta_1, \beta_2) &= \frac{1}{2 \sin(\beta_1 + \beta_2)} \left\{ \text{Im} \left[\text{Li}_2\left(\frac{\sin(\beta_1 + \beta_2)}{\sin\beta_1} e^{-i\beta_2}\right) + \text{Li}_2\left(\frac{\sin(\beta_1 + \beta_2)}{\sin\beta_2} e^{-i\beta_1}\right) \right] \right. \\ &\quad + 2 \text{Li}_2\left(\frac{1 - e^{-2i(\beta_1 + \beta_2)}}{2}\right) - \text{Li}_2(-e^{-2i(\beta_1 + \beta_2)}) \Big] \\ &\quad + (\beta_1 - \beta_2) \log \frac{\sin\beta_2}{\sin\beta_1} + \pi \log \frac{\sin^2(\beta_1 + \beta_2)}{\sin\beta_1 \sin\beta_2} \\ &\quad \left. + 2\left(\pi \Theta(\beta_1 + \beta_2 - \frac{\pi}{2}) - \beta_1 - \beta_2\right) \log \sin(\beta_1 + \beta_2) \right\}. \end{aligned} \quad (98)$$

¹⁷The results, obtained by performing the integrations in the chosen order, confess the symmetry in the β_j only after using some functional relations. For convenience we have written (98) in an obviously symmetrised manner.

$$\begin{aligned}
Q_{\text{oppo}}^{\text{planar}}(\beta_1, \beta_2) &= \left\{ \text{Im Li}_2\left(\frac{\sin|\beta_1 - \beta_2|}{\sin \max(\beta_1, \beta_2)} e^{i \min(\beta_1, \beta_2)}\right) - \frac{1}{2} \text{Im Li}_2\left(-e^{-2i|\beta_1 - \beta_2|}\right) \right. \\
&+ \text{Im Li}_2\left(\frac{1 - e^{-2i|\beta_1 - \beta_2|}}{2}\right) + \min(\beta_1, \beta_2) \log \frac{\sin \min(\beta_1, \beta_2)}{\sin \max(\beta_1, \beta_2)} \\
&\left. + \left(\pi \Theta(|\beta_1 - \beta_2| - \frac{\pi}{2}) - |\beta_1 - \beta_2|\right) \log \sin|\beta_1 - \beta_2| \right\} \frac{1}{\sin|\beta_1 - \beta_2|} .
\end{aligned} \tag{99}$$

Plots of these two functions are shown in fig.8. Both show runaway behaviour at some locations. In the same side case it is related to the approach to a situation with crossing edges at $\beta_1 + \beta_2 = \pi$, and at $\beta_1 + \beta_2 = 0$ it is necessary to fit the smooth contour case ($\alpha = \pi$) as discussed around (30). In the opposite side case the last comment also explains the singularity along the line $\beta_1 = \beta_2$. To understand the singularities along $\beta_1 = \pi$ and $\beta_2 = \pi$, one has to realise that if one of the β_j is equal to π , the corresponding edge is a piece of the circumcircle passing also the endpoint of the other edge.

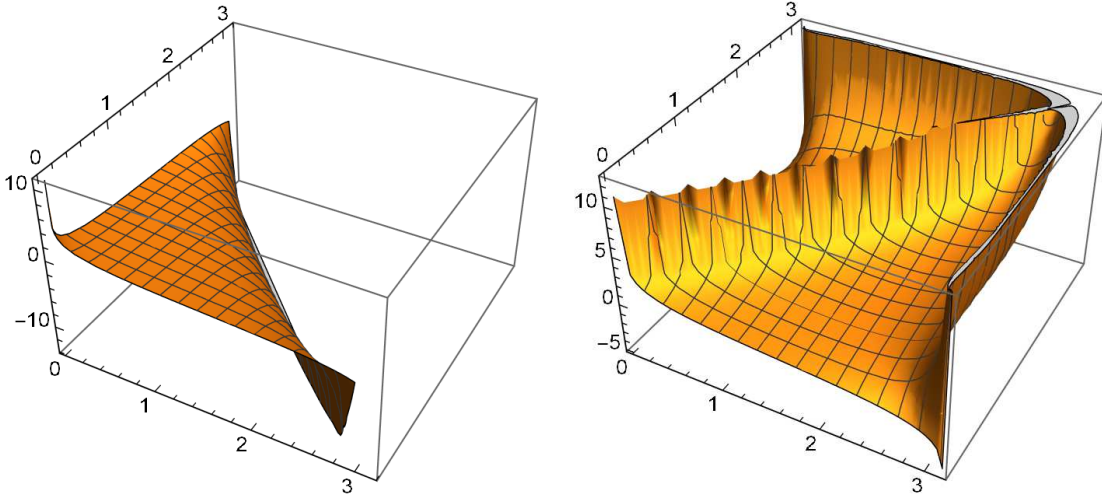


Figure 8: *On the left:* $Q_{\text{same}}^{\text{planar}}(\beta_1, \beta_2)$ for $\beta_1 + \beta_2 < \pi$. *On the right:* $Q_{\text{oppo}}^{\text{planar}}(\beta_1, \beta_2)$ for all $\beta_1, \beta_2 \in (0, \pi)$.

For e.g. $0 < \beta_2 < \pi$ and $\beta_1 \rightarrow 0$ the two planar versions of Q should coincide, since this just corresponds to the smooth transition between a same side and an opposite side situation. Indeed one finds

$$\begin{aligned}
Q_{\text{same}}^{\text{planar}}(0, \beta_2) &= Q_{\text{oppo}}^{\text{planar}}(0, \beta_2) \\
&= \frac{1}{\sin \beta_2} \left\{ \text{Im Li}_2\left(\frac{1 - e^{-2i\beta_2}}{2}\right) - \frac{1}{2} \text{Im Li}_2\left(-e^{-2i\beta_2}\right) \right. \\
&\quad \left. + \left(\pi \Theta(\beta_2 - \frac{\pi}{2}) - \beta_2\right) \log \sin \beta_2 \right\} .
\end{aligned} \tag{100}$$

References

- [1] H. Dorn, JHEP **03** (2020), 166 doi:10.1007/JHEP03(2020)166 [arXiv:2001.03391 [hep-th]].
- [2] L. F. Alday and J. M. Maldacena, JHEP **06** (2007), 064 doi:10.1088/1126-6708/2007/06/064 [arXiv:0705.0303 [hep-th]].
- [3] J. M. Drummond, G. P. Korchemsky and E. Sokatchev, Nucl. Phys. B **795** (2008), 385-408 doi:10.1016/j.nuclphysb.2007.11.041 [arXiv:0707.0243 [hep-th]].
- [4] N. Drukker, S. Giombi, R. Ricci and D. Trancanelli, JHEP **05** (2008), 017 doi:10.1088/1126-6708/2008/05/017 [arXiv:0711.3226 [hep-th]].
- [5] A. Cavaglià, N. Gromov and F. Levkovich-Maslyuk, JHEP **10** (2018), 060 doi:10.1007/JHEP10(2018)060 [arXiv:1802.04237 [hep-th]].
- [6] Y. He, C. Huang and M. Kruczenski, JHEP **02** (2018), 027 doi:10.1007/JHEP02(2018)027 [arXiv:1712.06269 [hep-th]].
- [7] G. S. Bali, Phys. Rept. **343** (2001), 1-136 doi:10.1016/S0370-1573(00)00079-X [arXiv:hep-ph/0001312 [hep-ph]].
- [8] D. S. Kuzmenko and Y. A. Simonov, Phys. Atom. Nucl. **66** (2003), 950-954 doi:10.1134/1.1577917 [arXiv:hep-ph/0202277 [hep-ph]].
- [9] O. Andreev, Phys. Rev. D **93** (2016) no.10, 105014 doi:10.1103/PhysRevD.93.105014 [arXiv:1511.03484 [hep-ph]].
- [10] P. V. Pobylitsa, JHEP **04** (2020), 204 doi:10.1007/JHEP04(2020)204 [arXiv:1908.01724 [hep-th]].
- [11] A. M. Polyakov, Nucl. Phys. B **164** (1980), 171-188 doi:10.1016/0550-3213(80)90507-6
- [12] N. Drukker, D. J. Gross and H. Ooguri, Phys. Rev. D **60** (1999), 125006 doi:10.1103/PhysRevD.60.125006 [arXiv:hep-th/9904191 [hep-th]].
- [13] H. Dorn, JHEP **03** (2018), 124 [erratum: JHEP **05** (2018), 108] doi:10.1007/JHEP03(2018)124 [arXiv:1801.10367 [hep-th]].
- [14] G. Cairns, R. Sharpe, and L. Webb, Rocky Mountain J. Math. Volume 24, Number 3 (1994), 933-959.
- [15] L. F. Alday, D. Gaiotto and J. Maldacena, JHEP **09** (2011), 032 doi:10.1007/JHEP09(2011)032 [arXiv:0911.4708 [hep-th]].
- [16] H. Dorn, H. Münkler and C. Spielvogel, Phys. Part. Nucl. **45** (2014) no.4, 692-703 doi:10.1134/S1063779614040066 [arXiv:1211.5537 [hep-th]].
- [17] N. Drukker and D. J. Gross, J. Math. Phys. **42** (2001), 2896-2914 doi:10.1063/1.1372177 [arXiv:hep-th/0010274 [hep-th]].